Materials and Design 85 (2015) 752–761

Contents lists available at ScienceDirect

Materials and Design

journal homepage: www.elsevier.com/locate/jmad

Investigation of mechanical and corrosion properties of an Al–Zn–Mg–Cu alloy under various ageing conditions and interface analysis of η′ precipitate

Wenchao Yang [a,c,d,*], Shouxun Ji [c], Qian Zhang [b], Mingpu Wang [d]

[a] State Key Laboratory of Solidification Processing, Northwestern Polytechnical University, Xi'an 710072, China
[b] Gränges Aluminium Co., Ltd., Shanghai 201807, China
[c] Brunel Centre for Advanced Solidification Technology (BCAST), Brunel University London, Uxbridge UB8 3PH, UK
[d] School of Materials Science and Engineering, Central South University, Hunan, Changsha 410083, China

ARTICLE INFO

Article history:
Received 21 March 2015
Received in revised form 9 June 2015
Accepted 23 June 2015
Available online 15 July 2015

Keywords:
Aluminium alloys
Microstructure
Ageing
Corrosion resistance
Interface analysis

ABSTRACT

The mechanical and corrosion properties under various ageing treatment conditions were investigated in an Al–6.0Zn–2.3Mg–1.8Cu–0.1Zr (wt.%) alloy. The results showed that the retrogression and re-ageing (RRA) were capable of providing higher strength and improved corrosion resistance in comparison with the conventional T6 and T74 ageing. The optimised ageing process had been found to be 120 °C/24 h + 180 °C/60 min + 120 °C/24 h for the experimental alloy. The results obtained from the high resolution transmission electron microscopy (HRTEM) interface analysis revealed that a semi-coherent stress field between the η′ precipitate and the Al matrix was critical in controlling the strength of the Al–Zn–Mg–Cu alloy heat-treated under different conditions. Furthermore, Transition Matrix calculation showed that the η′ phases had only two zone axes: $[\bar{1}\,2\bar{1}3]_{\eta'}$ and $[10\bar{8}\,2\,3]_{\eta'}$, which were parallel to the $[112]_{Al}$ zone axis, when being precipitated from the Al matrix. Therefore, the orientation relationships between the η′ precipitates and the Al matrix under the $[112]_{Al}$ zone axis could be described as: $[\bar{1}\,2\bar{1}3]_{\eta'}//[112]_{Al}$;$(1\bar{2}\,12)_{\eta'}//(1\bar{1})_{Al}$ and $[10\bar{8}\,2\,3]_{\eta'}//[112]_{Al}$;$(1\bar{2}\,12)_{\eta'}//(11\bar{1})_{Al}$. Consequently, a new diffraction pattern model from η′ precipitates in two variants under the $[112]_{Al}$ zone axis had been established, which was in a good agreement with the experimental data.

1. Introduction

The application of aluminium alloys in motor vehicles and other types of transportation equipment is becoming one of the most important ways to reduce structural weight, which can effectively lower fuel consumption and improve vehicle performance [1,2]. The combination of the relatively low mass of aluminium alloys with the improved strength, flexibility and other performance is essential to achieve light-weighting in transport structure [3,4]. Therefore, the aluminium alloys and the associated processing techniques need to be developed to maximise the performance while maintaining minimum costs.

The strengthening of the heat-treatable wrought Al–Zn–Mg–Cu aluminium alloy is predominately determined by the type and size of precipitates [5–7]. The precipitation sequence is usually described as: supersaturated solid solution → GP zones → η′ phase → η phase. The GP zones are generally formed during a natural ageing or in the early stage of an artificial ageing, which serve as nucleation sites for the formation of metastable η′ phase. It has been found that the metastable η′ phase, rather than the stable η phase ($MgZn_2$), is solely responsible for the peak hardening of Al–Zn–Mg–Cu alloys [8].

However, in the wrought Al–Zn–Mg–Cu alloys, the corrosion resistance is generally not sufficiently good to satisfy the industrial requirements. Moreover, the high strength and the satisfied corrosion resistance are difficult to achieve in the same time because the alloys are always sensitive to local corrosions including the intergranular corrosion, exfoliation corrosion and stress corrosion cracking (SCC) [9,10]. However, both the strength and the corrosion resistance of the alloy are equally important in application and these are closely associated with the microstructural characteristics, in particular the size and distribution of precipitates and precipitate-free zone (PFZ) at the grain boundaries [11,12]. Therefore, in order to obtain a combination of good corrosion resistance and improved strength, the microstructural control of the precipitates in the primary aluminium grains and at grain boundaries becomes essential for Al–Zn–Mg–Cu alloys. It is known that the heat treatment is an effective approach to modify the microstructure of wrought aluminium alloys. However, the commonly used T6 treatment can improve the strength, but worsen the local corrosion resistance [13]. On the other hand, several over-aged treatment processes such as T73, T74 and T76 have been developed recently to improve the corrosion resistance of aluminium alloys [14,

* Corresponding author at: State Key Laboratory of Solidification Processing, Northwestern Polytechnical University, Xi"an 710072, China. Tel./fax: +86 29 88492228.
E-mail address: yangwenchao1985@163.com (W. Yang).

http://dx.doi.org/10.1016/j.matdes.2015.06.183
0264-1275/

15]. Unfortunately, the alloy strength was simultaneously decreased by 5%–15% after applying these ageing processes. On the other hand, a retrogression and re-ageing (RRA) treatment was developed [16] to be able to obtain good corrosion resistance without significantly sacrificing the strength through forming fine precipitates inside the primary grains and coarse precipitates at grain boundaries [17,18]. Although the precipitates of η′ phase have been widely studied for Al–Zn–Mg–Cu alloys [5,19,20]. However, the strengthening mechanism of metastable η′ phase is still not fully understood in Al–Zn–Mg–Cu alloys, in particular, limited information can be found for the orientation relationships and interface structure of η′ phase.

Therefore, in the present study, we attempted to systematically investigate the effect of various ageing treatments on mechanical properties and corrosion behaviour of an Al–Zn–Mg–Cu alloy. And, the corresponding microstructure under various ageing treatment conditions was further studied by scanning electron microscopy (SEM) and transmission electron microscopy (TEM). And, the polarisation curves were used to analyse the corrosion behaviour of experimental alloys under the various ageing treatments. Furthermore, based on the microstructures, the crystallographic interface and morphology of the η′ precipitates under the $[112]_{Al}$ zone axis were analysed and discussed by means of the Transform Matrix calculation and the Fourier filtering technique. Finally, a new diffraction pattern model for η′ phase was established in the $[112]_{Al}$ zone axis.

2. Experimental

The Al–6.0Zn–2.3Mg–1.8Cu–0.1Zr (wt.%) alloy was used as starting materials with a sample size of 20 × 20 × 2 mm. The samples were solution-treated at 470 °C for 1 h in a salt bath furnace, followed by immediate quenching into cold water to room temperature. Then, the samples undergone various ageing treatment conditions including T6, T74 and RRA to investigate the mechanical properties, corrosion performance and microstructure. The details of the ageing processes were listed in Table 1.

Mechanical property test was performed on smooth plate specimens by an Instron 3369 testing machine at room temperature with a tensile speed of 2 mm/min. The gauge length and width of the specimen were 25 mm and 6 mm, respectively. The intergranular corrosion test was performed according to the standard of GB7998-2005 [21]. The corrosion medium was the solution of 57 g/L NaCl + 10 mol/L H_2O_2, and the testing temperature was 35 ± 1 °C. After 6 h immersion in the corrosion medium, the samples were cleaned and sectioned perpendicular to a corroded surface, followed by standard grinding and polishing. Then, the maximum intergranular corrosion depth was measured to evaluate the corrosion performance. Furthermore, the accelerated exfoliation corrosion test was performed at room temperature according to the EXCO test method described in ASTM G34-01 [22]. The EXCO test solution consisted of 4.0 mol/L NaCl + 0.5 mol/L KNO_3 + 0.1 mol/L HNO_3 at 0.4 pH. The electrolyte volume–electrode surface area ratio was 15 mL/cm^2. After 48 h immersion in the EXCO solution, the corrosion morphologies with various ageing treatments were recorded. The slow strain rate test (SSRT) in air and in a 3.5 wt.% NaCl water solution was carried out to investigate the SCC resistance according to GB 15970.7–2000 with a strain rate of 10^{-6} s^{-1} [23].

Table 1
Details of the heat treatment processes used for the experimental Al–Zn–Mg–Cu alloy.

Temper	Heat treatment process
T6	470 °C/1 h + water quench + 120 °C/6 h
T74	470 °C/1 h + water quench + 120 °C/6 h + 160 °C/16 h
RRA40	470 °C/1 h + water quench + 120 °C/24 h + 180 °C/40 min + 120 °C/24 h
RRA60	470 °C/1 h + water quench + 120 °C/24 h + 180 °C/60 min + 120 °C/24 h

FEI Sirion 200 SEM was used to observe the fracture morphology. Typical specimens at various ageing treatment conditions were selected for the detailed TEM and high resolution transmission electron microscopy (HRTEM) examinations. The specimens for TEM were prepared by a standard electro-polishing procedure. The electrolytic solution was a mixture of nitric acid and methyl alcohol (1:4). The electrolytic polishing was operated at 22 V from −20 °C to −30 °C. A JEOL-2100F HRTEM was used for the microstructural investigation.

3. Results

3.1. Effects of heat treatments on the strength

Fig. 1 presented the mechanical properties of the experimental alloy under various ageing treatment conditions. For the T6 temper sample, the ultimate tensile strength (UTS) and yield strength (YS) were 572 MPa and 489 MPa, respectively. Compared with the T6 temper, the UTS and YS of the T74 temper sample decreased 11.2% and 3.7%, respectively. The UTS and YS of the RRA40/RRA60 temper samples were 574 Mpa/577 MPa and 510 Mpa/513 MPa, respectively. Both of them were slightly higher than that of T6 temper but significantly higher than that of T74 temper. In conclusion, the strength was in the following order: RRA60 > RRA40 > T6 > T74.

3.2. Microstructures with the various heat treatment conditions

Fig. 2 showed the bright-field TEM images and the corresponding selected area diffraction patterns (SADPs) of the Al–Zn–Mg–Cu alloy with different heat treatment conditions under the $<112>_{Al}$ zone axis. In the T6 sample in Fig. 2a, it was observed that a large number of fine precipitates with 2–5 nm size were homogeneously distributed in the Al matrix. The SADP was shown in Fig. 2b. Except the diffraction spots from the Al matrix, some weak diffraction streaks were also observed at the 1/3 and 2/3 220_{Al} positions, which indicated that the fine η′ phases had been precipitated [24], although they were not predominate in the microstructure. Generally, the combination of GP zones and η′ phase resulted in the strengthening at T6 heat treatment [7]. At the same time, some precipitates were also observed at the grain boundaries with a continuous distribution. The precipitates at the grain boundaries were 4–10 nm in size, implying the formation of the equilibrium η phase.

Fig. 2c and d represented the TEM images and the corresponding SADP of the T74 sample. Compared with the microstructure obtained under T6 treatment, the precipitates obtained by T74 treatment were coarser with about 10–20 nm size in the matrix. However, it was obvious that the precipitates presented a discontinuous distribution along grain

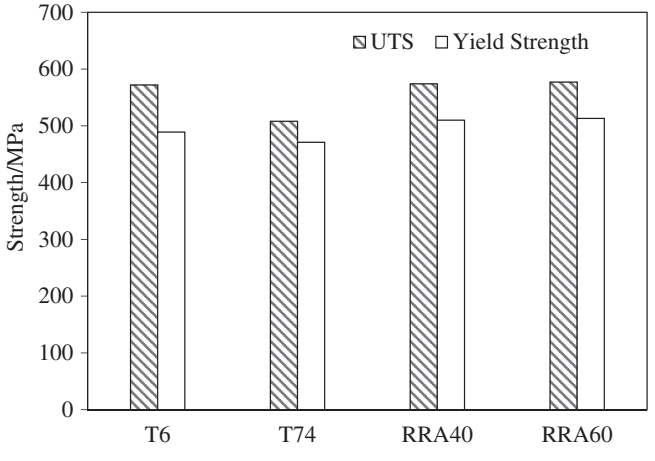

Fig. 1. Mechanical properties of the experimental alloy various ageing treatment conditions.